Supporting Information

Fabrication of Solution-Processed Low Voltage TFT By Using Colloid 2D ZnO Nanosheets and its application as a UV photodetector

Abhik Bhuin[a‡], Akhilesh Kumar Yadav[b‡], Utkarsh Pandey[b], Debdyuti Mukherjee[c], Vivek Kumar Agrahari [d], Caroline Ponraj[a], Subha Sadhu*[d], Bhola Nath Pal*[b], Sujoy Sarkar*[e]

a Department of Physics, School of Advanced Sciences, Vellore Institute of Technology Chennai, Vandalur-Kelambakkam Road, Chennai-600127, Tamil Nadu, India

b School of Materials Science and Technology, IIT BHU, Banaras Hindu University Campus, Varanasi, Uttar Pradesh 221005 India

c Centre for Fuel Cell Technology (CFCT), International Advanced Research Centre for Powder Metallurgy and New Materials (ARCI), IIT-M Research Park, Taramani, Chennai 600113

d Department of Chemistry, Institute of Science, Banaras Hindu University, Varanasi - Uttar Pradesh 221005 India 221005

e Department of Chemistry, SAS & Electric Vehicle Incubation, Testing and Research Centre (EVIT-RC), Vellore Institute of Technology Chennai, Vandalur-Kelambakkam Road, Chennai-600127, Tamil Nadu, India

*Email: subha@bhu.ac.in; bnpal.mst@itbhu.ac.in; sujoy.sarkar@vit.ac.in

‡ These authors contributed equally

List of supplementary figures

Figure S4. a) Valence Band XPS spectrum of ZnO NS; b) XPS survey spectrum.

Figure S5. Capacitance vs. frequency curve of $LiInSnO_4$ dielectric.

Figure S6. (a) XRD and AFM images (b) 2D and (c) 3D of $LiInSnO_4$ dielectric, Cross-sectional SEM image of (d) $LiInSnO_4$, mixed ZnO Nanosheets annealed at (b) 110 ˚C and (f) 350 ˚C tin films.

Figure S7. Histogram for the statistical analysis of the TFT parameters mobility, threshold voltage, and subthreshold swing.

Figure S8. Transmittance Vs Wavelength (b) Tauc's plot of LiInSnO4 dielectric.

Figure S9. Output characteristics of reference devices at different Temperatures.

Figure S10. Transfer characteristics under UV light illumination.

Figure S11. Transient photo response

Figure S12. External quantum efficiency

Figure S13. Voltage vs Intensity variation under UV illumination.

Figure S14. Transient response of the devices under prolonged UV illumination.

Table S1: Comparison table of synthesis methods and corresponding morphology of ZnO NPs

Table S2: TFT Parameters of Devices

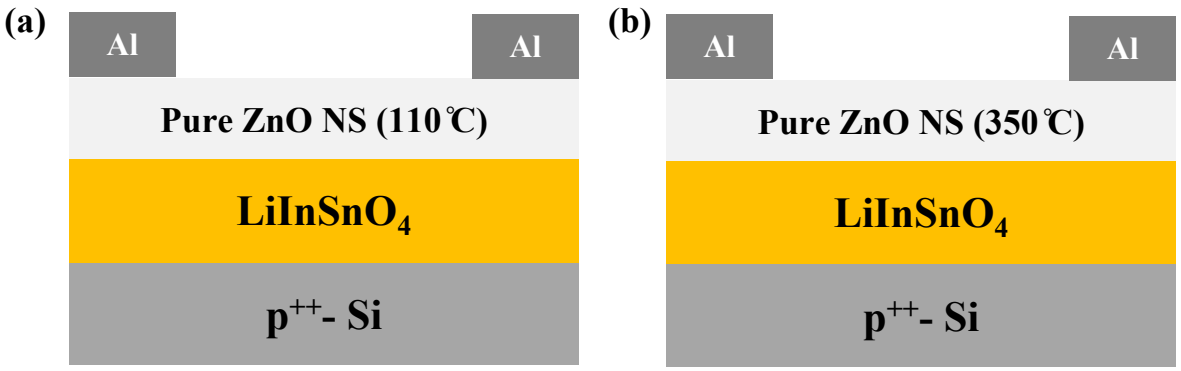

Figure S1. Schematic representation of solution-processed TFT's (p^{++}-Si/$LiInSnO_4$/ ZnO NS) with semiconducting layer processed at (a) A-R (110 C) (b) B-R (350 C).

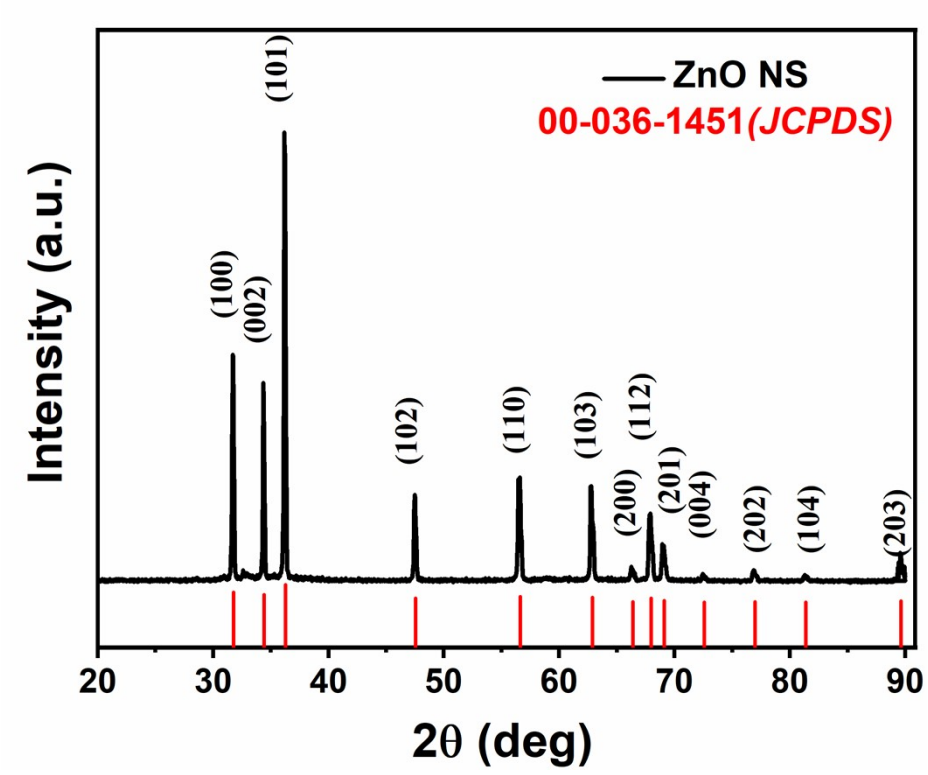

Figure S2. p-XRD pattern of as-synthesized ZnO NS along with JCPDS card no. (00-036-1451).

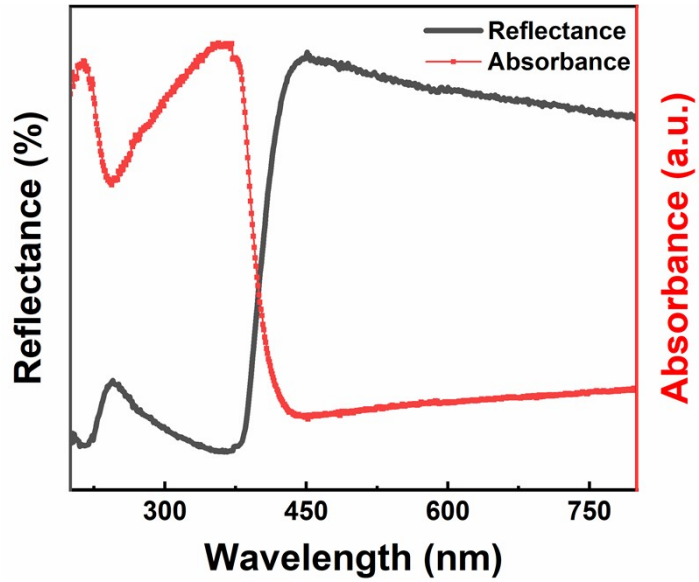

Figure S3. UV-vis absorbance and reflectance spectra of as-synthesized ZnO NS.

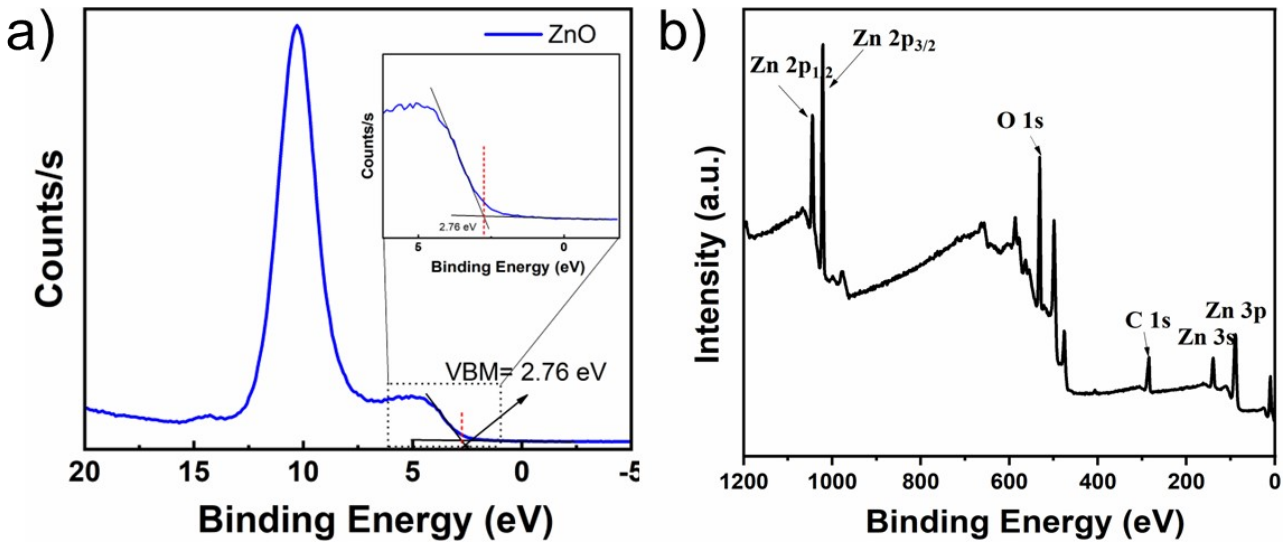

Figure S4. a) Valence band XPS spectra of bulk ZnO. The inset shows a detailed XPS spectrum near the valence band maximum; b) XPS survey spectrum of ZnO NS.

$$E_{CBM}=E_{VBM}-E_g = 2.76 - 3.2= -0.44 \text{ eV}$$

Dielectric characterisation

The Frequency-dependent capacitance (C–f) of the dielectric thin film was studied using the same MIM devices within a frequency range of 20 Hz to 1 MHz. It is noteworthy that the areal capacitance of the film at lower frequencies is high (>200 nF/cm²), which can be seen in Fig. S4(a), which is suitable for low operating voltage TFTs, making it an excellent choice for reducing the operating voltage of TFTs. Moreover, the areal capacitance of the dielectric is ~ 180 nF/cm2 at 50 Hz frequency. To assess the electrical properties of the solution-processed $LiInSnO_4$ single-layer, a device was fabricated with a metal-insulator-metal (MIM) structure. The current–voltage (I−V) characteristics of this device demonstrate that the current density for the single-layer dielectrics is significantly low, attributed to the large optical bandgap (5.3 eV) of the $LiInSnO_4$ thin film.

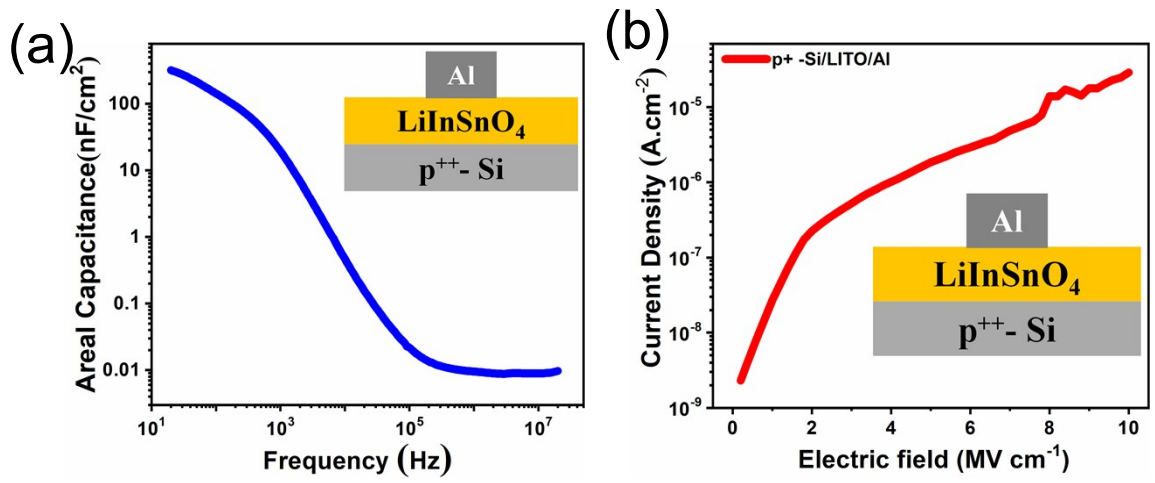

Figure S5. a) Capacitance vs. frequency curve of $LiInSnO_4$ dielectric, and b) Leakage current vs. Electric field curve of the $LiInSnO_4$ dielectric in MIM structure.

The current density of the $LiInSnO_4$ thin film is notably higher under an applied voltage exceeding 1.0 V (10^{-8} A/cm²). As depicted in Fig. S4(b), the current density of the single-layer $LiInSnO_4$ dielectric, annealed at 550 °C, is approximately (10^{-8} A/cm²). Under an applied voltage of ~2 V. Furthermore, it was observed that both devices remain stable up to an 8 V external bias, indicating that these dielectric thin films can safely operate up to an 8 V

voltage. This stability suggests a low pinhole density in the dielectric thin film, which is essential for high-performance thin-film transistors (TFTs). Overall, these findings indicate that solution-processed $LiInSnO_4$ ionic dielectrics are promising candidates for use as gate dielectrics in TFT fabrication.

Structural Properties

Grazing incidence X-ray diffraction (GIXRD) measurement has been performed to confirm the crystalline phase of the $LiInSnO_4$ dielectric thin film annealed at 550º C on a silicon substrate, Shown in Figure S5a. There is no visible peak has been observed in the GIXRD pattern of the LITO dielectric thin film confirming the amorphic nature. The AFM of $LiInSnO_4$ ion-conducting dielectric is performed as shown in Fig. S5(b) and the 3D view in Fig. S5(c) leads to extracted root mean square (RMS) surface roughness of dielectric thin film is 0.406 nm, shows the smoothness of the dielectric thin film. This film has the potency to make smooth conduction of carriers at the dielectric/semiconductor interface and helps to increase the mobility of the carriers.

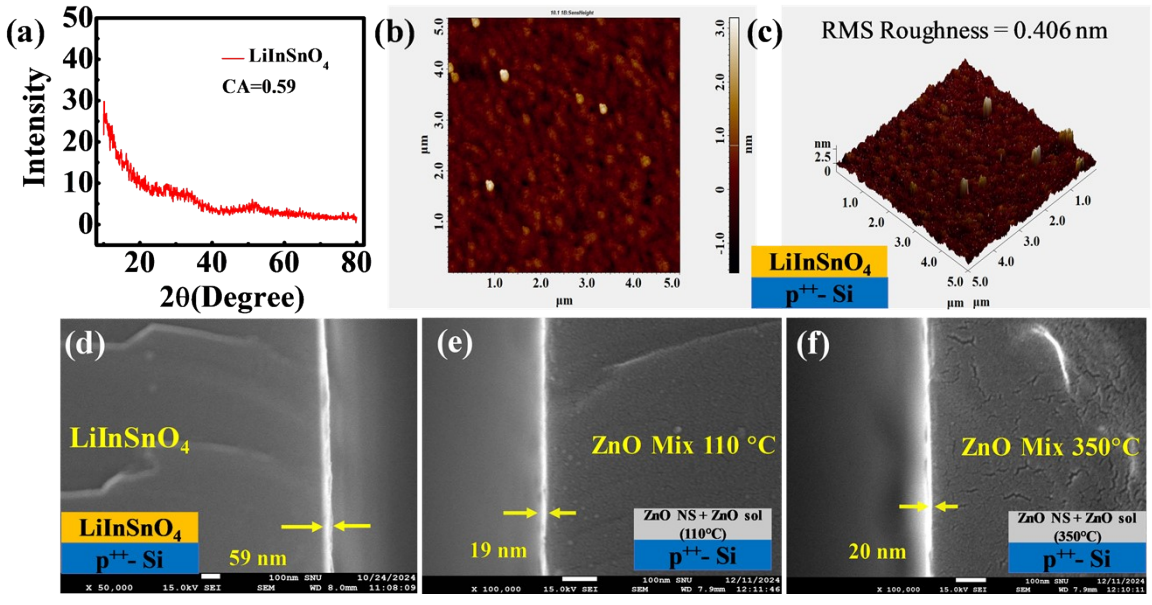

Figure S6. (a) XRD pattern for $LiInSnO_4$. AFM images (b) 2D and (c) 3D of $LiInSnO_4$ dielectric thin film (p^{++}-Si/ $LiInSnO_4$) with R_{rms} ~ 0.406 nm. The cross-sectional SEM images of the thin film of (d) $LiInSnO_4$ and mixed ZnO Nanosheets annealed at (e) 110 ℃ and (f) 350 ℃.

Moreover, the cross-sectional SEM images of the $LiInSnO_4$ dielectric layer and the ZnO Nanosheets film annealed at 110 C and 350 C, presented in Figure S6(d), S6(e) and S6(f), respectively. The estimated thicknesses of the $LiInSnO_4$ layer are 59 nm and the ZnO mixed film annealed at 110 C and 350 C are 19 nm and 20 nm, respectively.

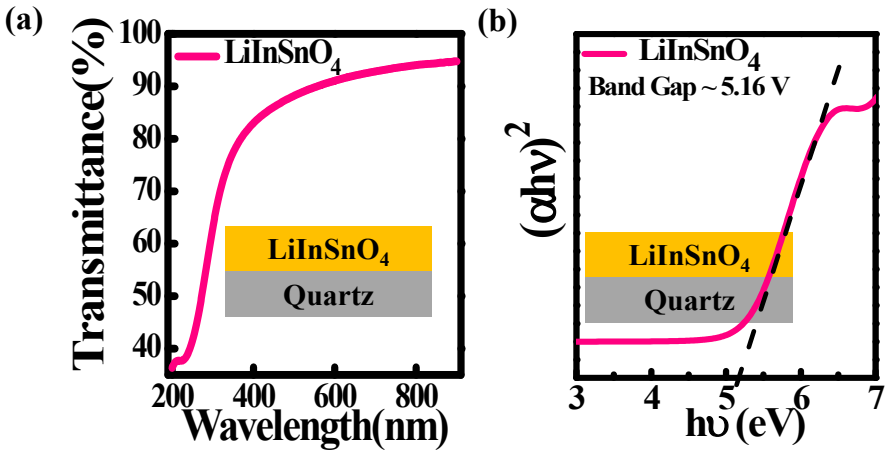

Figure S7. (a) Transmittance Vs Wavelength (b) Tauc's plot of $LiInSnO_4$ dielectric.

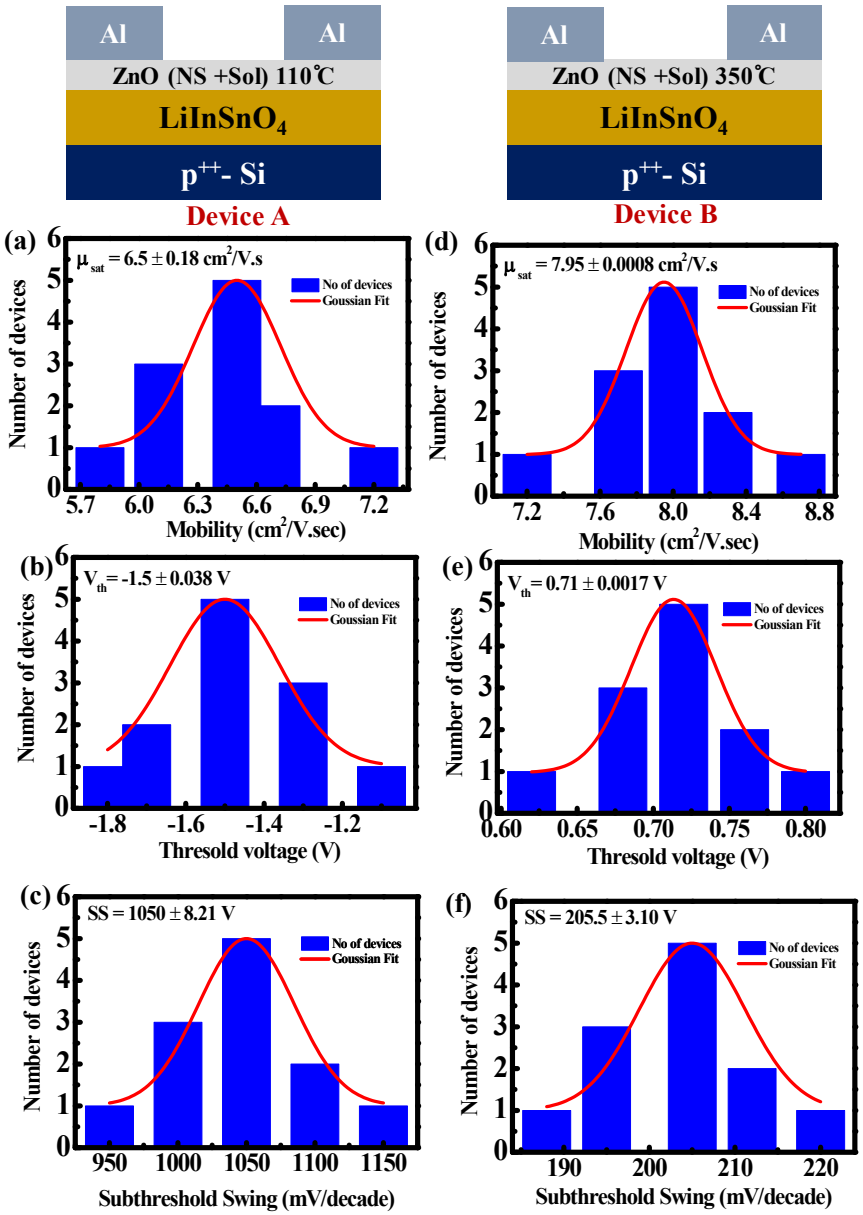

Figure S8. Histogram for statistical analysis of Device A (a) mobility, (b) threshold voltage (Vth), and (c) subthreshold swing (SS), while (d), (e), and (f) for Device B.

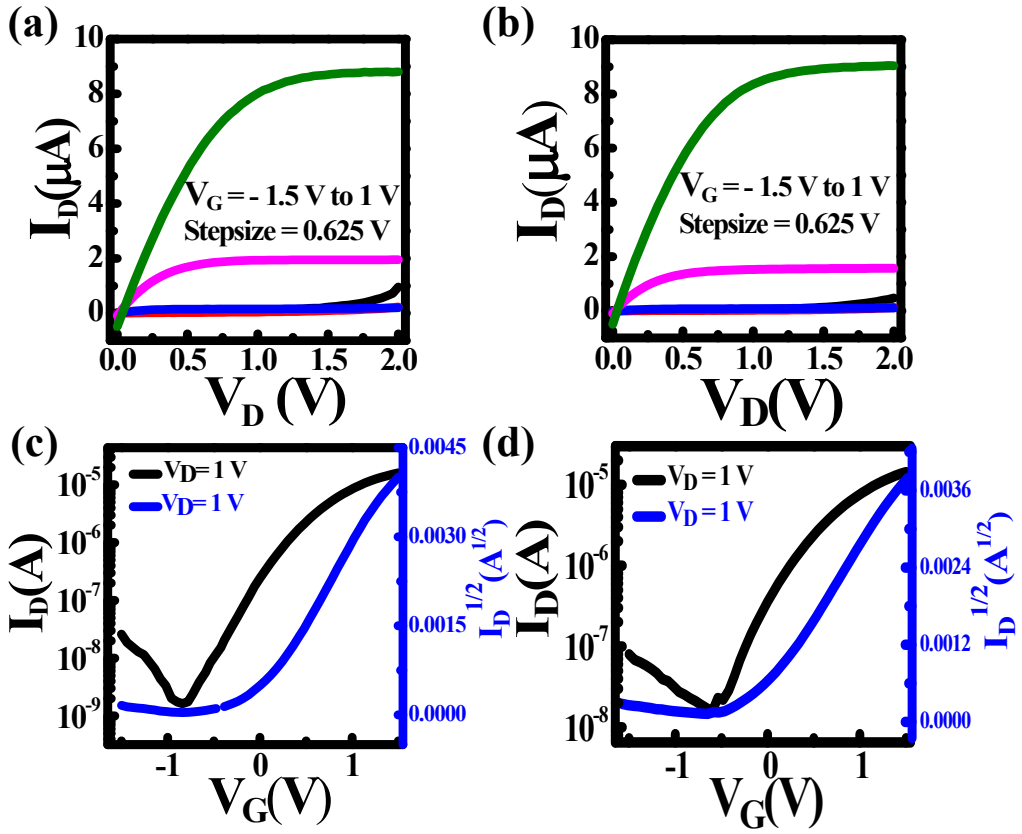

Figure S9. Output characteristics of reference devices a) A-R (110 C) b B-R (350 C) and Transfer Characteristics of reference devices c) A-R (110 d) B-R (350 C).

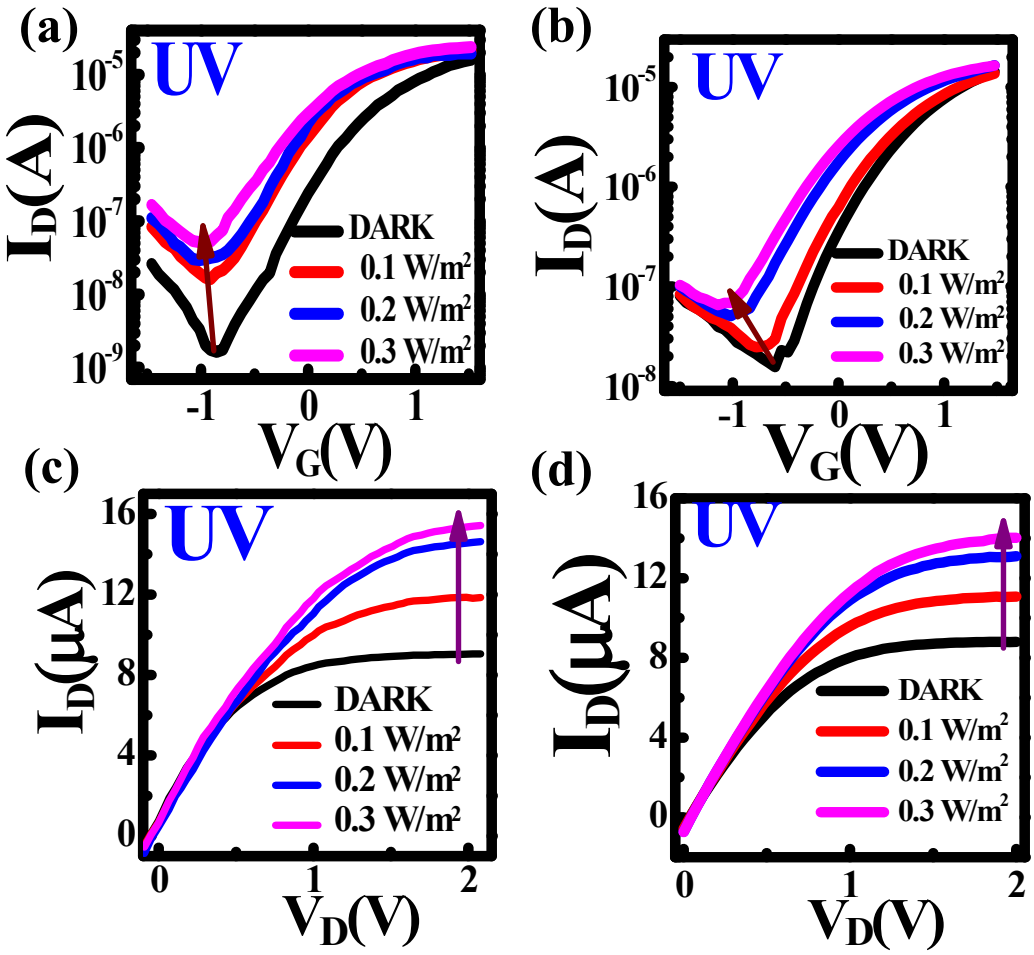

Figure S10. Transfer characteristics under UV light illumination of (a) A-R (110 C), (b) B-R (350 C) and Output characteristics under UV light illumination of (c) A-R (110 d) B-R (350 C), under UV illumination.

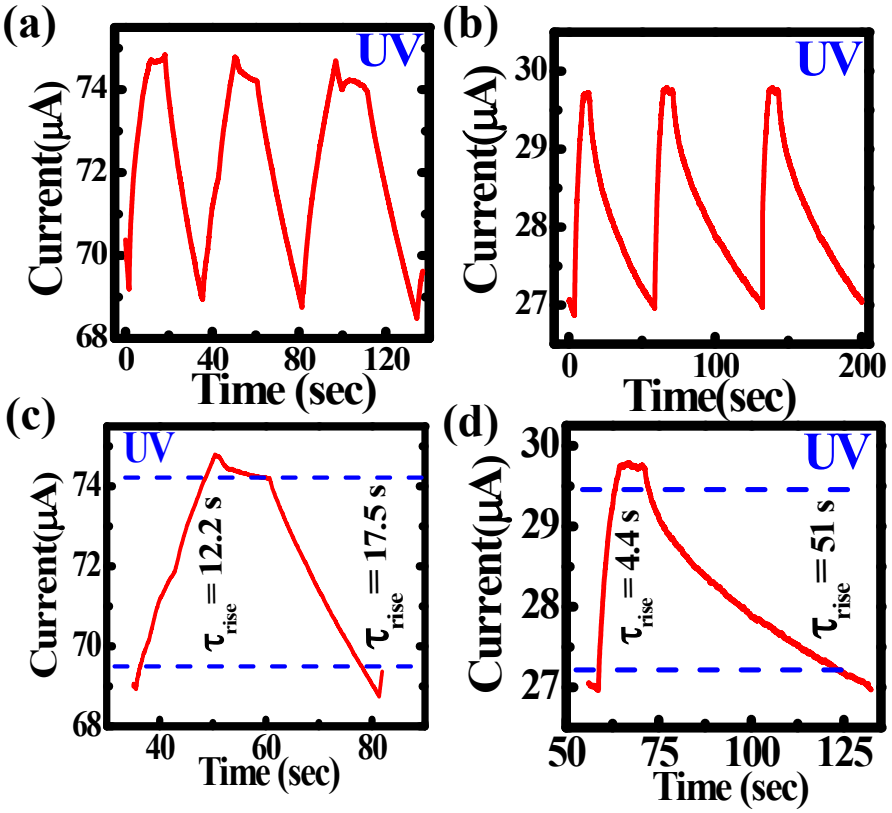

Figure S11. Transient photo response of (a) A-R (110 C) (b) B-R (350 C) under UV illumination, and corresponding single cycles of (c) A-R (110 C) (d) B-R (350 C).

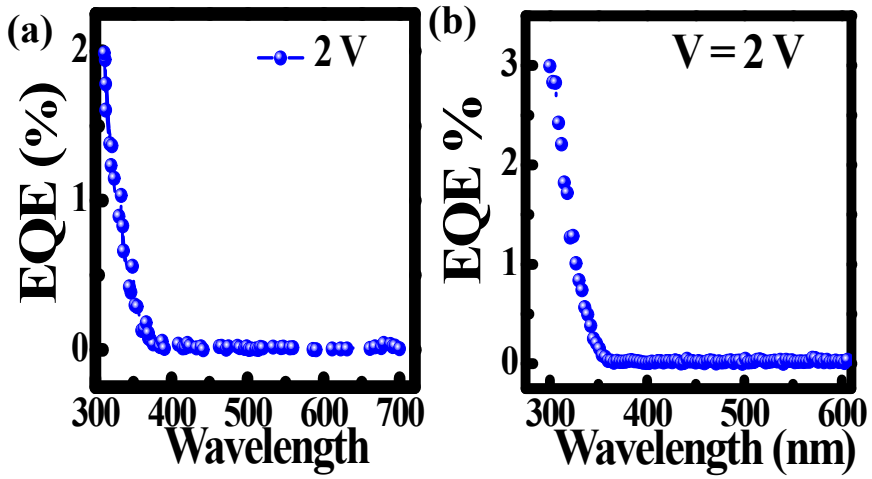

Figure S12. External quantum efficiency of (a) Device A-R (110 C) and (b) Device B-R (350 C).

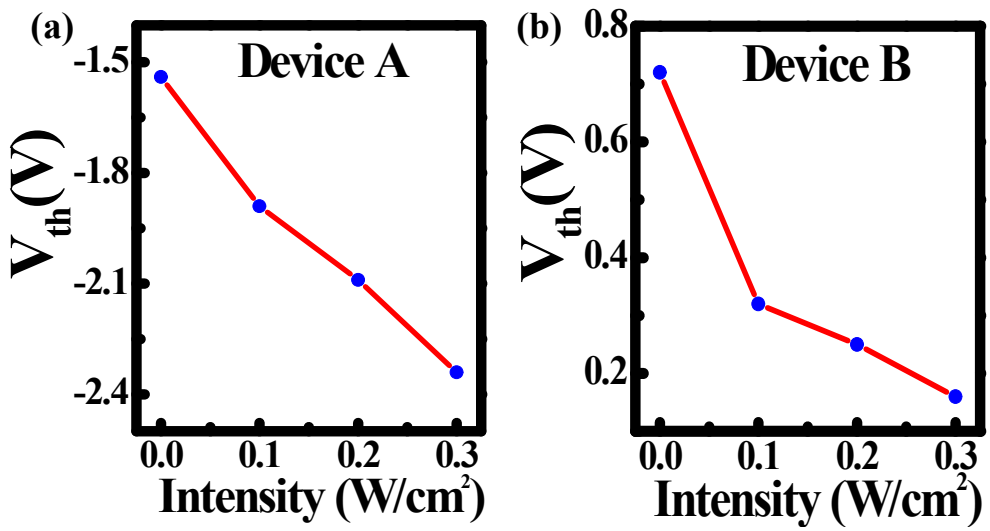

Figure S13. Voltage v/s Intensity variation of (a) Device A, (b) Device B, under UV illumination.

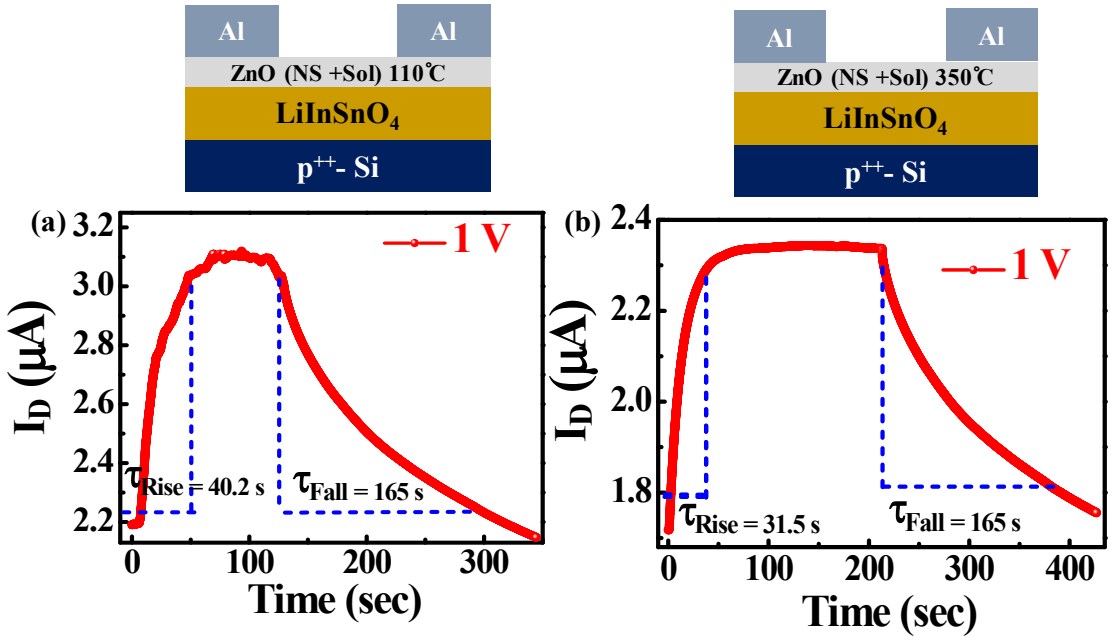

Figure S14. Transient response under prolonged UV illumination of 0.3 W/m^2 of (a) Device A and (b) Device B.

Table S1: Comparison table of synthesis methods and corresponding morphology of ZnO

Strategy	Morphology	Dimension	Crystalline Size from XRD	Particle Size from SEM	Particle Thickness	
Konjac glucomannan template	Porous Nanoclusters	-	22-25 nm		-	[1]
Graphitic carbon nanofibers (GCNF)	Hollow tubular + Agglomerated Particles	3D	31-56 nm	50nm-90nm	-	[2]
China rose petal	hierarchical ZnO	-	-	-	-	[3]
Sodium dodecyl sulfate (SDS) as surfactant	Nanosheets	2D	40.3 nm			[4]
Fructose as surfactant	Nanodrums	-	44 nm	-	-	[4]
Cetrimonium Bromide (CTAB) as surfactant	Nanoneedles	1D	49.6 nm	-	-	[4]
Tween 80 as surfactant	nano granular		20 nm	20-30 nm	-	[5]
Oleic acid as surfactant	flower-like nano rod		24 nm	20-30 nm	-	[5]
Gluconic acid as surfactant	nanoflakes assembled hierarchical structure,		23 nm	20-30 nm	-	[5]
CTAB as surfactant	loosely aggregated structure		25 nm	26 nm	-	[6]
PEG as surfactant	loosely aggregated structure		27 nm	28 nm	-	[6]
Azadirachta indica (Neem leaf) extract	-		25.95 and 33.20 nm	10-70 nm	-	[7]
This Work	nanosheet	2D	56 nm	200 nm	30 nm	

Table S2. TFT Parameters of Device A-R and B-R

Device Configuration	On/Off ratio	Subthreshold Swing (mV/decade)	Mobility ($cm^2/V.\ s$)	Threshold voltage V_{th}(V)	Number of trap states N. (Cm^{-1})
Device A-R (110°C)	**1.1×10^4**	**366**	**0.50**	**-0.03**	**$6.1\ X\ 10^{12}$**
Device B-R (350°C)	**1.0×10^3**	**382**	**0.34**	**-0.14**	**$6.4\ X\ 10^{12}$**

References

1 Liu, B., Ding, J., Chen, H. & Fu, H. Konjac glucomannan template based synthesis of porous ZnO nanostructures for enhanced ethanolamine gas detection. *Chemical Physics* **591**, 112596 (2025).

2 Dillip, G. R., Banerjee, A. N. & Joo, S. W. Template-Based Synthesis of Hollow Nanotubular ZnO Structures and Nonlinear Electrical Properties under Field-Induced Trap-Assisted Tunneling. *The Journal of Physical Chemistry C* **124**, 28371-28386 (2020).

3 Jiao, C., Tang, F. & Xue, M. Template synthesis of porous nanoZnO and its adsorption capability. *Micro & Nano Letters* **12**, 466-469 (2017).

4 Iqbal, T. *et al.* Surfactant assisted synthesis of ZnO nanostructures using atmospheric pressure microplasma electrochemical process with antibacterial applications. *Materials Science and Engineering: B* **228**, 153-159 (2018).

5 Zare, M. *et al.* Surfactant assisted solvothermal synthesis of ZnO nanoparticles and study of their antimicrobial and antioxidant properties. *Journal of Materials Science & Technology* **34**, 1035-1043 (2018).

6 Kumar, D., Singh, R. & Gautam, M. Impact of surfactant-assisted synthesis on the structural, optical, and dielectric characteristics of ZnO nanoparticles. *Nano Express* **5**, 015002 (2024).

7 Haque, M. J., Bellah, M. M., Hassan, M. R. & Rahman, S. Synthesis of ZnO nanoparticles by two different methods & comparison of their structural, antibacterial, photocatalytic and optical properties. *Nano Express* **1**, 010007 (2020).